# NUMERICAL STUDY OF LIQUID-SOLID SEPARATION PROCESS INSIDE THE HYDROCYCLONES WHIT DIFFERENT GENERATRIX OF THE CONE

## IPATE GEORGE, CASANDROIU TUDOR

University "POLITEHNICA" of Bucharest

**Abstract**: Hydrocyclones are getting more and more interest from various industries. They are widely used to separate particles from liquid. Modeling of complex and multiphase flow behavior inside the hydrocyclone is done usually with the help of computational fluid dynamic study. Current study involves numerical investigation of separation performance characteristics of the hydrocyclone using new design parameters. The Reynolds averaged Navier–Stokes equation employing k–e turbulence model were solved to calculate the turbulent flow field in a hydrocyclone. The particle trajectories were computed by integrating the force balance equations on particles based on the predicted flow field. The separation efficiency defined as the fraction of particles recovered to underflow was obtained by using the calculated particle trajectories.

**Keywords:** simulation, hydrocyclones, centrifugal separator, efficiency separation.

### 1. INTRODUCTION

Hydrocyclone is a device which is used for the separation of materials contained in the liquid fed into it. These materials are normally in the form of solid particles, but they may also be the gas bubbles, oil, or others. The suspended particles are separated from the liquid due to the centrifugal force induced inside the hydrocyclone. Unlike centrifuges that use the same separation principle, hydrocyclones have no moving parts and the necessary vortex motion is performed by the liquid itself. Hydrocyclone geometry and operating parameters can be calculated based on the empirical or semi-empirical equations as reviewed by Svarovsky (1984) and Chen et al. (2000),[1,2]. These equations can be used to predict the performance of hydrocyclones and make the proper selections, but have their limitations due to the specific system on which the correlation development was based. Therefore, it is important to understand the fluid flow and its effect on particle separation in order to improve the performance of hydrocyclone. With the advance in computational fluid dynamics, many numerical works on the flow patterns inside hydrocyclones emerged (Michael D. Brayshaw, 1990; Hsieh and Rajamani, 1991; Monrendon et al., 1992; Dyakowski and Williams, 1993; P. He, M. Salcudean and I.S. Gartshore, 1999), [3,4,5,6,7]. Although previous authors assumed that the flow was axisymmetric and the relevant twodimensional equations were solved, the inlet conditions are clearly not axisymmetric for commercial hydrocyclones. Threedimensional computational works to simulate the flows in hydrocyclones were reported in recent years (A.F. Nowakowski, 2003; Yang et al., 2004; Th. Neesse and J. Dueck., 2004; Jose A. Delgadillo et al., 2007; B. Wang et al., 2008), [6,7,8,9,10,11,12].

It is the purpose of the present work to study the feasibility of hydrocyclone process for the thickening of sludge in water purifying plants, since the classical process adopted for sludge thickening in water purifying plants may require more space and longer processing time to produce high sludge concentration than hydrocyclone process.

In order to attain the purpose, a three-dimensional simulation was performed to predict the flow field and the separation efficiency in hydrocyclones whit different geometry of cone.

#### 2. MATHEMATICAL MODEL

To model a highly turbulent fluid flow in a hydrocyclone, Reynolds averaged continuity and Reynolds averaged Navier–Stokes equations were solved. They can be written in Cartesian component form as follows,[12]:

$$\frac{\partial u_i}{\partial x_i} = 0 \tag{1}$$

$$\rho \left( \frac{\partial u_i}{\partial t} + u_j \frac{\partial u_i}{\partial x_i} \right) = -\frac{\partial P}{\partial x_i} + \frac{\partial}{\partial x_j} \left[ \mu \left( \frac{\partial u_i}{\partial x_j} + \frac{\partial u_j}{\partial x_i} \right) - \rho \overrightarrow{u_i u_j} \right] + \rho g_i$$
 (2)

where  $u_i$  is the fluid velocity component,  $x_i$  is the Cartesian coordinate component,  $\rho$  is the fluid density, t is the time, P is the pressure,  $\mu$  is the fluid viscosity, and  $g_i$  is the component of gravitational acceleration vector. The term,  $\rho u_i^* u_j^*$ , of Eq. (2) is often termed the Reynolds stress and represents the effects of the turbulent velocity fluctuations on the mean flow. By analogy with the molecular diffusion of momentum, the Boussinesq hypothesis (Hinze, 1975),[13], relates the turbulent momentum transport to the gradients of the mean velocity field. The Reynolds stress in Eq. (2) is then expressed by,[14]

$$-\rho \overline{u_i^{\prime} u_j^{\prime}} = \mu_t \left( \frac{\partial u_i}{\partial x_j} + \frac{\partial u_j}{\partial x_i} \right) - \frac{2}{3} \left( \rho k + \mu_t \frac{\partial u_i}{\partial x_j} \right) \delta_{ij}$$
(3)

where  $\mu_t$  is the turbulent viscosity, k is the turbulent kinetic energy,  $\delta_{ij}$  is the Kronecker delta. The turbulent viscosity is related directly to the turbulent kinetic energy and the viscous dissipation,  $\epsilon$ , as

$$\mu_{t} = \rho C_{\mu} \frac{k^{2}}{\varepsilon} \tag{4}$$

where  $C_{\mu}$ =0.0845, derived from renormalization group (RNG) methods (Choudhury, 1993),[15].

In order to calculate the trajectories of the particles, it was assumed that the effect of the motions of particles on the flow and the particle/particle interactions not are negligible for a dense sludge considered in the present study. The particles were regarded as rigid spheres. Then, the computation of the particle trajectories can be carried out independently, once the flow field of the liquid phase is obtained. Based on the Newton's second law of motion, the equation of motion for the particle is written as,[16]

$$\frac{\pi d^3 \rho_p}{6} \frac{dv_p}{dt} = \frac{1}{8} \pi \rho_f d^2 \left| v_f - v_p \right| \left( v_f - v_p \right) + F_b - \frac{\pi d^3}{6} \left( \rho_p - \rho_f \right) \omega \times \left( \omega \times \bar{R} \right) - \frac{\pi d^3 \rho_p}{3} \omega \times v_p \quad (5)$$

equation who represent the particle transport model implemented in ANSYS CFX, where  $\rho$  is the density of the particle, v is the velocity vector of the particle, and first term is the drag force  $F_d$ , second term  $F_b$  represent buoyant force, third term is centrifugal force  $F_c$ , and last term denote inertial forces  $F_i$  exerted on the particle, respectively. Subscript p and p refers to the solid, respectively fluid particles. The expressions for the above forces can be found in He et al. (1999), Ipate et al.(2007), [7,17]. Eq. (5) is an ordinary differential equation for the particle velocity vector,  $v_p$ , with respect to time. To obtain  $v_p$ , Eq. (5) has to be integrated with time. The trajectories of the particles can be found by integrating  $v_p$  with respect to time once again. Equation are available in flows where the particle density is much greater than the fluid density, where the particle inertia is related to

the instantaneous difference in velocity between the particle and the fluid, and the rotational and external body forces.

#### 3. NUMERICAL SIMULATIONS

To illustrate how the optimized computer model can be used for engineering design, simulations were performed for a hydrocyclone with modified geometry. The numerical prediction results for the different designs are compared in the following discussion. To investigate the influence behavior of geometry on the hydrocyclone performance in more details, hydrocyclones with common type cone, parabola type cone and hyperbola type cone were designed as illustrated in Fig. 1. Except the shape of the cone, other geometric parameters of these hydrocyclones were all the same. The lengths of the cone sections were all 1085 mm. For the parabola type cone, the generatrix equation was designed as follows:

$$Y_p = 0.037 \cdot r^2 + 4.084 \cdot r - 110.778 \tag{6}$$

where, the coordinate center was chosen at the center of the smaller end of cone part; Y stands for the axial position (mm); and r for the radial position (mm). For the hyperbola type cone, the equation of the generatrix was designed as:

$$Y_h = 1830 \cdot r^3 - 0.502 \cdot r^2 + 49.843 \cdot r - 873.51 \tag{7}$$

Simulations were performed for mean particle diameters of 131.2, 116.6, 109.3, 111.6, 111.9 and 112.1  $\mu m$  and cone radius of 2.6 and 25.0 cm. The liquid phase was water, the density of the solid particles was 2.65 g/cm<sup>3</sup> and the particle size was distributed broadly from 5  $\mu m$  to 400  $\mu m$ . The solid concentration of feed was between 9.7-13.2 % by volume. The flow rates of feed, overflow, and underflow were 280.92, 186.91, and 93.28 kg/ min, respectively, in numerical simulations presented below. The solid weight concentrations and the particle size distributions of the samples were also calculated.

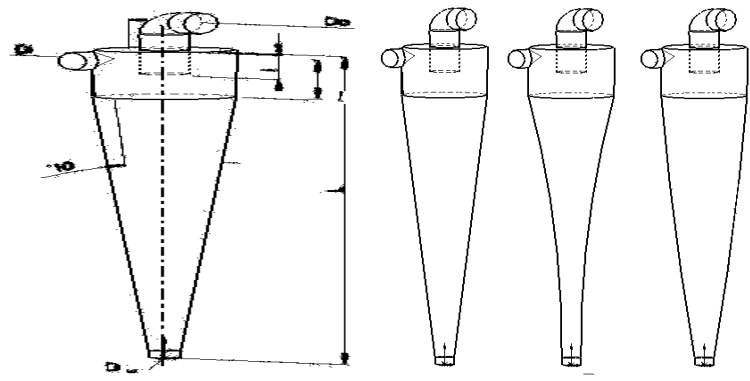


Fig. 1 Ilustration of the hydrocyclone characteristic and geometry

The geometry of the hydrocyclones used in the simulation is shown in Fig. 1 and Table 1.

Geometric characteristic of hydrocyclones - Table 1

$D_{c}$	D <sub>i</sub> /D <sub>c</sub>	D <sub>o</sub> /D <sub>c</sub>	D <sub>u</sub> /D <sub>c</sub>	1/D <sub>c</sub>	L/D <sub>c</sub>	Cone angle degree
250 mm	0.28	0.34	0.2	0.4	5	10

The flow field in a hydrocyclone was obtained by using a commercial computational fluid dynamics code ANSYS CFX, which employs the finite volume method (Ansys ,2005), [18]. The finite volume mesh used for the calculation is shown in Fig. 2. A total of 51460 tetrahedrons having 9712 nodes and 3314 faces were used for the mesh cone type, 50971 tetrahedrons having 9617 nodes and 3266 faces for the parabola mesh type,

respectively, 52380 tetrahedrons having 9926 nodes and 3516 faces for the hyperbola mesh type. Calculations were performed on Notebook Dell Inspiron 1501. The computation time required for a converged solution was approximately 0.5 h. The calculated contour plot of the axial components of the pressure is shown in Fig. 3.

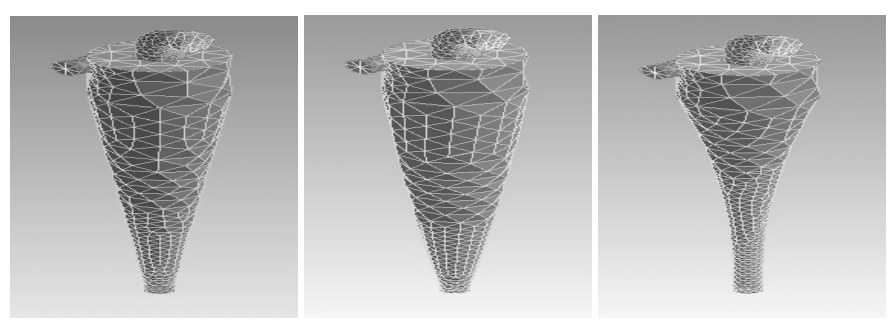


Fig. 2 Finite volume meshes

To examine the combined effect of turbulence model and geometry type, results for the water velocity and curl water velocity at the three heights, y=1.085 y=0.655 and y=0.255 m, are presented in Figs. 4, 5 and 6. Radial position was nondimensionalized with respect to the hydrocyclone radius and velocity is nondimensionalized by the mean inlet velocity.

#### 4. RESULTS AND DISCUSSION

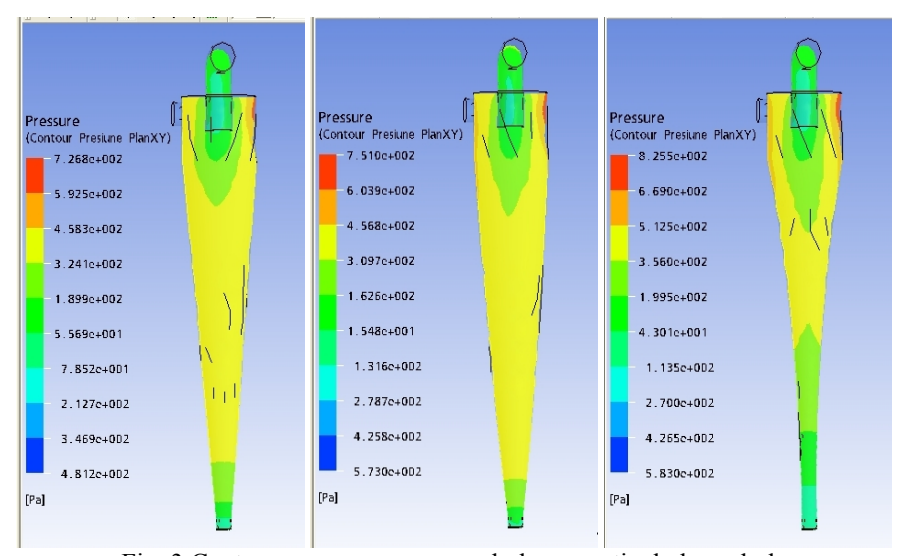


Fig. 3 Contour pressure-cone, parabola respectively hyperbola

The contour plots of the swirl component of the velocity and pressure are presented in Figs. 4, 5 and 6, respectively. Fig. 3 shows that the maximum pressure occurs in the cylindrical section near the feed inlet and the minimum pressure occurs near the underflow exit.

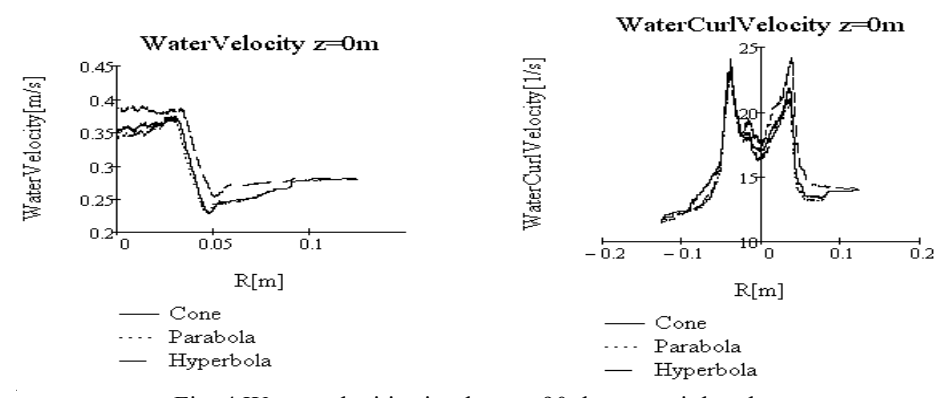


Fig. 4 Water velocities in plane at 90 degree to inlet plane

Since the pressure gradient balances the centrifugal force, a significant radial pressure variation exists near the exit of the underflow due to the strong swirl flow in that region as shown in Fig. 4. From Figs. 5–6, it can be clearly seen that the flow field is not axisymmetric. Fig. 4 shows that there is a recirculating flow of the liquid in the cylindrical section and the upper portion of the conical section, and thus the point of axial flow reversal occurs in the upper portion of the conical section rather than deep in the apex regions.

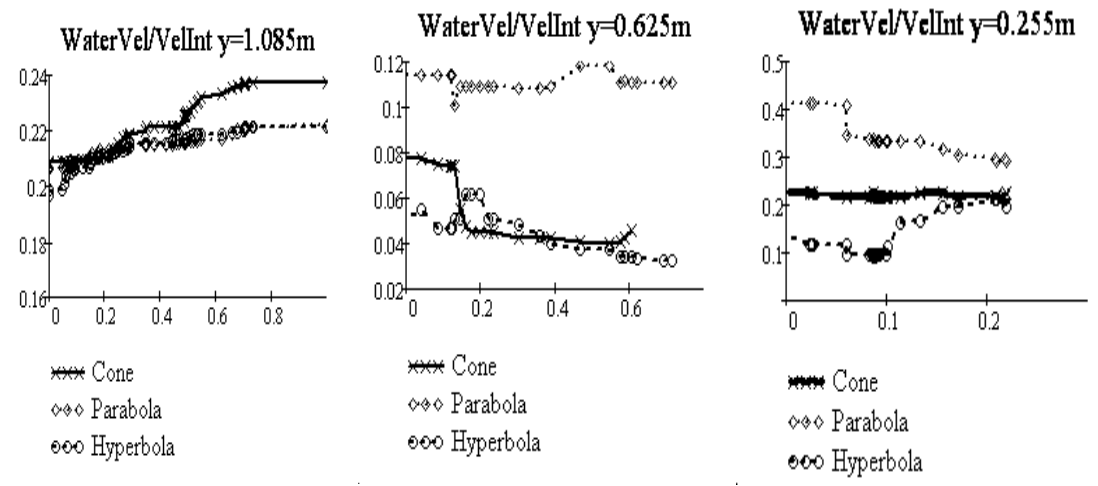


Fig. 5 Water velocities in XZ plane at different heights

Fig. 4 illustrates that the tangential component of the velocity increases to a maximum value close to the axis and then decreases toward the wall, as the radial distance from the axis increases.

Figure 7 shows fluid velocity vectors in diametral planes at circumferential angles of 90 deg from the inlet plane. These figures show the flow field to vary significantly with circumferential position. They also indicate the complicated structure of the velocity field in the hydrocyclone,[19,20,21].

Comparison of the pressure drop like difference between flow inlet pressure and overflow pressure is shown in Fig. 8. The figure show that the total pressure drop coefficient decreases when the cone diameter increases. There are probably two main factors contributing to this trend. Assuming that the discharge coefficient of the orifice remains approximately constant, maintaining the same flow rate through a smaller orifice diameter will lead to a higher pressure drop; conservation of angular momentum will require a higher tangential velocity of the vortex core and increase shear losses. The variation in the total pressure drop for different geometry is somewhat counter-intuitive. Figure 8 shows that the pressure drop across the hydrocyclone decreases with increasing cone radius, while experience from pipe flow suggested that the total pressure drop coefficient should increase with increasing pipe radius. The observed decrease with increasing cone radius is probably due to increasing diffusion

of the vortex core, which reduces the intensity of the secondary circulation such that the reduction in wall shear stress more than offsets the increase in surface area.

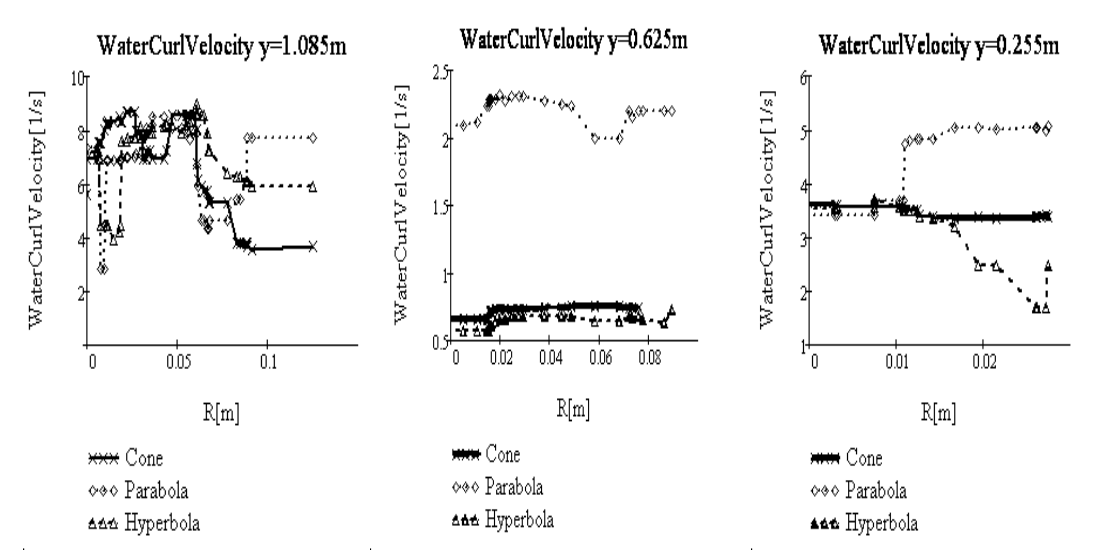


Fig. 6 Water Curl Velocity in XZ plane at different heights

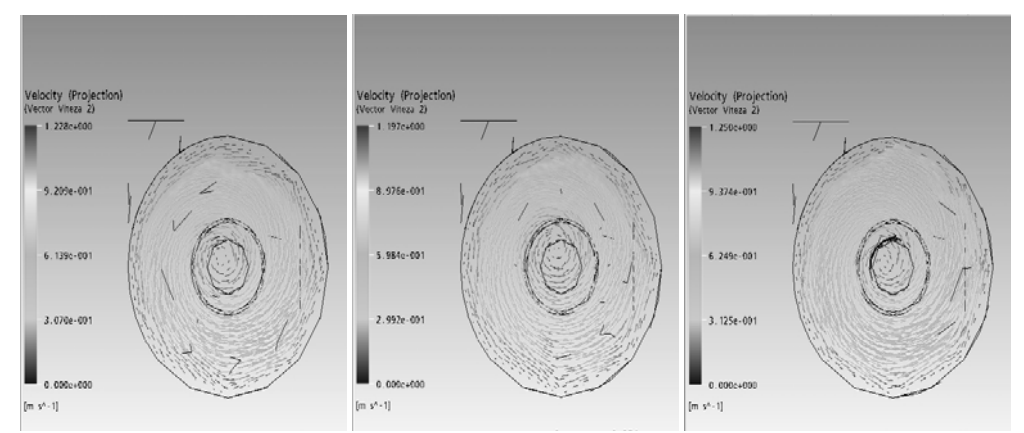


Fig. 7 Velocity vector plot in orizontal plane XZ at y=1.085 m

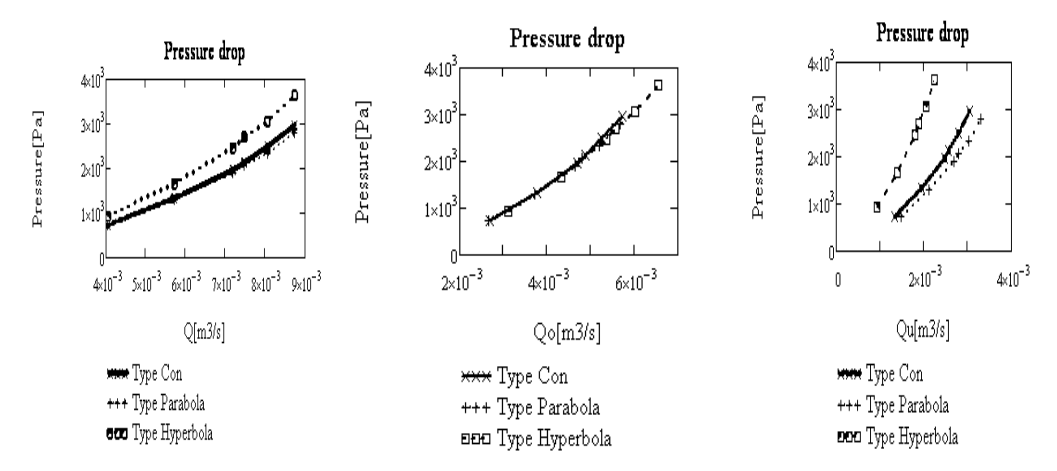


Fig. 8 Pressure drop across the hydrocyclone

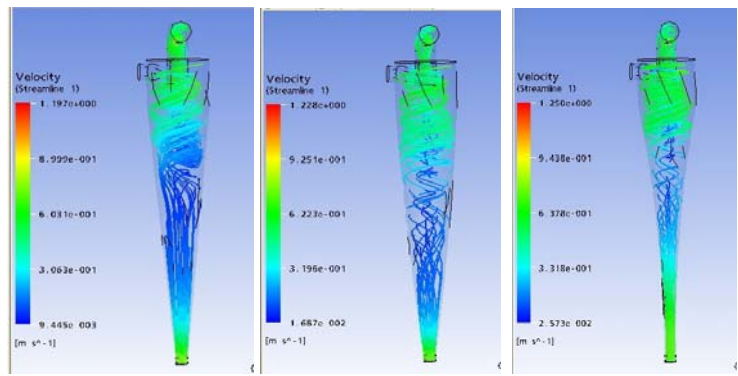


Fig. 9 Streamline of solid particles

The ultimate goal of the simulation is to predict the separation efficiency of the hydrocyclones. The total efficiency was calculated as the percentage of particles recovered to the underflow. Fig. 9 shows the computed trajectories of particles released at different positions, recovered to the underflow and to the overflow. In order to test the validity of the simulation, the calculated separation efficiency as a function of particle size was compared with the literature experimentally data. Although the calculation overestimates the separation efficiency for the particles with the diameter smaller than 50 µm and for those with the diameter of 125–135 µm, the calculated and measured separation efficiency curves are generally in good agreement, [22,23].

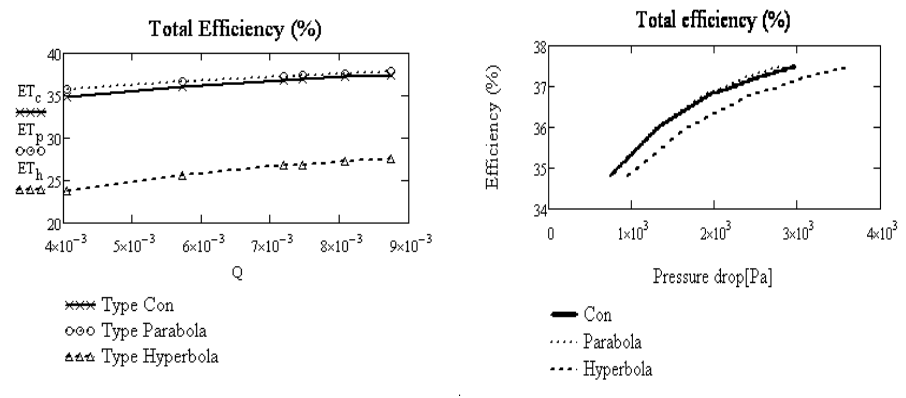


Fig. 10 Total efficiency in hydrocyclones

The effect of total inlet volumetric flow rate and pressure drop on the percentage separation of solid particles has been presented in Figs. 10. It can be seen from these figures that, with increase in volumetric flow rate, which is related to increase in velocity of the fluid flow inside the hydrocyclone, the efficiency of separation of solid particles increases. This may be due to increasing swirling in the hydrocyclone, which is also confirmed by the other researchers cited in the literature. Also from these figures can be seen that with increase in inlet volumetric flow rate, percentage removal of particles increases rapidly initially, after that separation percentage increase is very less. The reason may be because two opposite facts act on the particles. As increase in inlet volumetric flow rate is related to high velocity and due to which eddies formed around the vortex lead to lower efficiency of separation. This trend is observed for all three geometrical types' formation inside the hydrocyclone.

## 5. CONCLUSIONS

A three-dimensional simulation was performed to study the flow field in a hydrocyclone to be used for the sludge separation in water purifying plants. The particle trajectories were calculated to predict the separation efficiency of the hydrocyclone. The calculated separation efficiency agreed favorably with the literature experimental data. The simulation methodology presented in this study, which was validated through the comparison with the literature experimental data, may be a useful first step to the feasibility study of a hydrocyclone process to be used for the thickening of sludge in water purifying plants.

The results show that the modification of the geometry in hydrocyclone type hyperbola did not improve the classification performance, and they are not suitable for experimental validation. Design of hydrocyclone type parabola showed a very slower performance achieved with the standard designs. Design of the standard hdrocyclone will be excellent candidates for further experimental validation. The principal contribution of this paper is that the computational fluid dynamics is the right tool to study and explore novel designs of hydrocyclones.

#### **REFERENCES**

- [1]. Svarovsky, L., *Hydrocyclones*. Holt (Rinehart & Winston), New York, USA, (1984).
- [2]. Chen, W., Zydek, N., Parma, F., Evaluation of hydrocyclone models for practical applications. Chemical Engineering Journal 80, 295–303, (2000).
- [3]. Brayshaw M. D., A numerical model for the inviscid flow of a fluid in a hydrocyclone to demonstrate the effects of changes in the vorticity function of the flow field on particle classification, International Journal of Mineral Processing, 29, 51-75, (1990).
- [4]. Hsieh, K.T., Rajamani, R.K., Mathematical model of the hydrocyclone based on physics of fluid flow. AIChE Journal 37, 735–746, (1991).
- [5]. Monrendon, T.C., Hsieh, K.T., Rajamani, R.K., *Fluid flow model of the hydrocyclone: an investigation of device dimensions.* International Journal of Mineral Processing 35, 65–83, (1992).
- [6]. Dyakowski, T., Williams, R.A., *Modelling turbulent flow within a small-diameter hydrocyclone*. Chemical Engineering Science 48, 1143–1152, (1993).
- [7]. He, P., Salcudean, M., Gartshore, I.S., *A numerical simulation of hydrocyclones*. Transactions of the Institution of Chemical Engineers 77, 429–441, (1999).
- [8]. Nowakowski, A.F., Kraipech, W., Williams, R.A., Dyakowski, T., *The hydrodynamics of a hydrocyclone based on a threedimensional multi-continuum model*. Chemical Engineering Journal 80, 275–282, (2000).
- [9]. Yang I.H., Shin C.B., Kim T.-H., Kim S., A three-dimensional simulation of a hydrocyclone for the sludge separation in water purifying plants and comparison with experimental data, Minerals Engineering 17, 637–641 (2004).
- [10]. Neesse, Th., Dueck, J., Minkov, L., Separation of Finest Particles in Hydrocyclones, Minerals Engineering, Vol. 17, pp. 689-696, (2004).
- [11]. Delgadillo J.A., Rajamani R. K., *Exploration of hydrocyclone designs using computational fluid dynamics*, International Journal of Mineral Processing, 84, 252-261, (2007)
- [12]. Wang B., Yu A.B., Numerical study of the gas-liquid-solid flow in hydrocyclones with different configuration of vortex finder, Chemical Engineering Journal, 135, 33-42, (2008).
- [13]. Hinze, J.O., Turbulence, McGraw-Hill, New York, (1975).
- [14]. Jiao J., Zheng Y., Sunb G., Wang J., Study of the separation efficiency and the flow field of a dynamic cyclone, Separation and Purification Technology, 49, 157–166, (2006).
- [15]. Choudhury, D., *Introduction to the renormalization group method and turbulence modeling*. Fluent Inc. Technical Memorandum, TM-107, (1993).
- [16]. Ipate G., Casandroiu T., Computer simulation of liquid-solid separation hydrocyclone whit two conical sections, Modelling and optimization în the machines building field, 2, MOCM-13, Romanian Technical Sciences Academy, (2007).
- [17]. Ipate G., Casandroiu T., Numerical study of liquid-solid separation process inside the hydrocyclones whit double cone sections, Scientific Bulletin of U.P.B., 69, 19-28, (2007)
- [18]. ANSYS 10,. User's Guide. Fluent Inc., Berkeley, CA., (2005)
- [19]. Chua L.Y., Yua W., Wang G.J., Zhoua X.W., Chena W.M., Dai D.Q., Enhancement of hydrocyclone separation performance by eliminating the air core. Chemical Engineering and Processing 43, 1441–1448, 2004. [20]. Castilho, L.R. Medronho, R.A. A Simple Procedure for Design and Performance Prediction of Bradley and Rietema Hydrocyclones, Minerals Engineering, 13, (2), pp. 183-191, (2000).
- [21]. Dai, G.Q., Li, J.M., Chen, W.M., *Numerical prediction of the liquid flow within a hydrocyclone*. Chemical Engineering Journal 74, 217–223, (1999).
- [22]. Kawatra, S. K., Optimization of Comminution Circuit Throughput and Product Size Distribution by Simulation and Control, Final Technical Report, (2005).
- [23]. Richard A. Arterburn, *The sizing and selection of hydrocyclones*, Krebs Engineers, Menlo Park, CA, (1976).